A QM/MM Free Energy Study of the Oxidation Mechanism of Dihydroorotate Dehydrogenase (Class 1A) from Lactococcus lactis

ARTICLE *in* THE JOURNAL OF PHYSICAL CHEMISTRY B · JANUARY 2015

Impact Factor: 3.3 · DOI: 10.1021/jp512860r · Source: PubMed

3 AUTHORS, INCLUDING:

José Rogério Silva
Federal University of Pará
17 PUBLICATIONS **33** CITATIONS
SEE PROFILE

Adrian Roitberg
University of Florida
164 PUBLICATIONS **7,505** CITATIONS
SEE PROFILE

THE JOURNAL OF PHYSICAL CHEMISTRY B

Article

pubs.acs.org/JPCB

A QM/MM Free Energy Study of the Oxidation Mechanism of Dihydroorotate Dehydrogenase (Class 1A) from *Lactococcus lactis*

José Rogério A. Silva,[†,‡] Adrian E. Roitberg,*[,‡,§] and Cláudio Nahum Alves*[,†,‡]

[†]Laboratório de Planejamento e Desenvolvimento de Fármacos, Instituto de Ciências Exatas e Naturais, Universidade Federal do Pará, Belém, PA 66075-110, Brazil

[‡]Department of Chemistry, University of Florida, Gainesville, Florida 32611-7200, United States

[§]Quantum Theory Project, University of Florida, Gainesville, Florida 32611-8435, United States

Supporting Information

ABSTRACT: The dihydroorotate dehydrogenase (DHOD) class 1A enzyme catalyzes is the only redox enzyme in the biosynthetic pathway (de novo) of pyrimidines where dihydroorotate (DHO) is oxidized to orotate (OA) coupled to reduction of a flavin mononucleotide (FMN) cofactor. The rupture of two DHO C−H bonds can proceed in a concerted or stepwise way. Herein, the catalytic mechanism of DHOD from *Lactococcus lactis* involving DHO oxidation (first half-reaction) was described using a hybrid quantum mechanics/molecular mechanics (QM/MM) approach and molecular dynamics simulations. The free energy profile obtained from self-consistent charge−density functional tight binding/molecular mechanics calculations (corrected by DFT/MM) reveals that this occurs with the proton abstraction from DHO C_5 to Cys_{130} deprotonated and DHO H_6 is transferred to FMN N_5 in a concerted mechanism with a very low barrier of 5.64 kcal/mol. Finally, through a residual decomposition analysis, the residues that have the main influence on the redox reaction were identified.

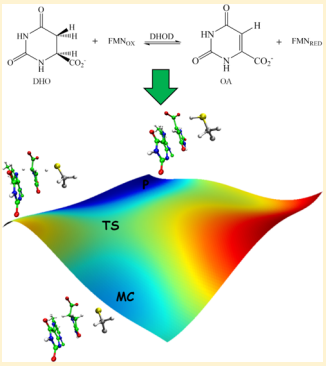

INTRODUCTION

Dihydroorotate dehydrogenase (DHOD)[1] is an enzyme acting in the de novo synthesis of pyrimidines. DHOD contains a flavin cofactor and is responsible for the only redox reaction in the pathway, making orotate (OA) from dihydroorotate (DHO) (Scheme 1). Because of the diversity of DHODs among different organisms,[2] compounds that selectively inhibit de novo pyrimidine biosynthesis can be developed for some organisms while not affecting others. Therefore, the DHOD enzyme represents an attractive and selective target for many diseases such as malaria, cancer, gastric ulcers, and rheumatoid arthritis.[3−6]

Scheme 1. Oxidation of DHO to ORO Catalyzed by a Class 1A DHOD Enzyme

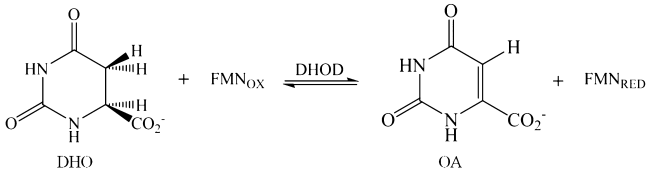

Inhibitors of human DHOD, such as the immunosuppressive drug leflunomide, have been used for the treatment of rheumatoid arthritis.[5,7,8]

DHODs can be divided into class 1 and class 2, based on sequence.[1] The class 1 enzymes are cytoplasmic proteins and have been further subdivided into subclasses 1A and 1B.[9,10] In the second half-reaction, the substrate fumarate (FUM), is reduced to succinate by the DHOD enzyme (a homodimer), a member of family 1A, using flavin mononucleotide (FMN) as a cofactor.[10] The class 1B enzymes are $\alpha_2\beta_2$ heterotetramers. They contain an iron−sulfur cluster and flavin adenine dinucleotide (FAD) cofactor[9] besides FMN (as all other DHODs). Class 2 DHODs enzymes are found as monomers or homodimers and are membrane-bound, using ubiquinone as cofactor.[11]

The mechanism of DHOD when dehydrogenating DHO has been studied extensively.[2,9,10,12−23] Two C−H bonds need to break when oxidizing DHO. An active site base (A serine in class 2 enzymes or a cysteine in class 1 enzymes) deprotonates carbon C_5 of DHO, while a hydride (or hydride equivalent) transfers from the C_6 of DHO to the N_5 of the middle ring of flavin. Most discussions of the mechanism center on the question of whether the scission of the two bond breaking events occurs in a concerted or stepwise manner.

By studying the class 1A DHOD from *T. cruzi* in complex with substrates and products of the first and second half-reactions, Inaoka and co-workers proposed a mechanism for two half-reactions.[24] Fagan proposed that the conversion of DHO to ORO on flavin reduction in anaerobic experiments occurs by concerted mechanism.[13]

Received: December 24, 2014
Revised: January 5, 2015
Published: January 7, 2015

DOI: 10.1021/jp512860r
J. Phys. Chem. B 2015, 119, 1468−1473

Recently, austin model 1/molecular mechanics (AM1/MM) simulations were used to study the mechanism of the half-reactions in the DHOD (class 1A) from *T. cruzi*.[19] We found that in the first half-reaction, the proton from the C_5 in DHO is transferred to a deprotonated Cys, followed by a hydride transfer from the C_6 DHO to the N_5 FMN. In this case, bond breakage and bond formation occurred in a stepwise manner.

Here, we have reported a computational study to elucidate which mechanism is acting in Class 1A of DHOD from *Lactococcus lactis* (*L. lactis*), applying a hybrid quantum mechanics/molecular mechanics (QM/MM) approach and molecular dynamics (MD) simulations.[25−37] In these calculations, a (small) part of the system is studied by QM while the rest is studied with an MM force field.[25,33,38] We used density functional tight binding (DFTB) in order to describe the QM part of the system. DFTB method has been shown to be very reliable in studying the energetics of chemical reactions,[37,39] correlating with higher levels of theory such as MP2.[40] A previous theoretical study has also shown that DFTB provides the best semiempirical description of deformation in six-membered carbohydrate rings.[41] The free energy surface (FES) for the catalytic reaction of DHO oxidation was computed via an umbrella sampling simulation. We also performed an analysis of the stabilization due to key residues inside the catalytic site on the transition state (TS) and the Michaelis complex (MC), using a residual decomposition analysis.

THEORETICAL METHODS

The System. The study started from the coordinates of *L. lactis* DHOD, downloaded from the PDB database and resolved at 2.00 Å (PDB code 2DOR).[2] The *L. lactis* DHOD system consists of 311 amino acid residues, 346 crystalline water molecules with the OA product and FMN cofactor bound in the active site. In our simulations, the OA product was changed, in silico, to the DHO substrate. We used the empirical propKa program[42] to assign the protonation states of all titratable amino acid residues at pH 7. Missing hydrogen atoms were added using the LEaP module of the AMBER12 package.[43] A truncated octahedral periodic box of TIP3P[44] water molecules was used for solvation with 10 Å on each side. The ff99SB[45] was used for the protein, while GAFF[46] was employed to describe the DHO substrate. The restrained electrostatic potential (RESP) procedure method at HF/6-31G* level of theory was used to assign the DHO charges using the Gaussian09 package.[47] The FMN cofactor was described using parameter files available in Bryce Group Web site.[48]

The starting system prepared as described previously was first minimized with 10 000 steps of a conjugate gradient algorithm, using the sander module of AMBER12 package. Then, the system gradually heated from 0 to 300 K over 2 ns constraining the solute with a force constant of 10 kcal/(mol·Å^2), followed by free equilibration for 200 ps before the production stage. All bonds between heavy atoms and hydrogens were restrained using the SHAKE algorithm.[49] We used a time step of 2 fs during for the MD simulations. A nonbonded cutoff of 8 Å with a PME implementation was used to calculate the long-range Coulomb Forces during all simulations.

The atoms of DHO, FMN, and Cys130 were included in the QM region, which contains 49 atoms. The SCC-DFTB method,[50] implemented in AMBER12,[51] was used to describe the QM region. The protein was described plus using the ff99SB[45] force field, while a TIP3P model was used for the water molecules. The link atom method was used[52] to saturate the valence of the QM/MM frontier.

QM/MM Umbrella Sampling and Potential Mean Force (PMF). The umbrella sampling was carried out using a linear combination of the distances described in Scheme 2. A two-dimensional (2D) PMF was obtained to explore the DHO oxidation in the mechanism of *L. lactis* DHOD. Two coordinates were defined for the sampling: RC1 = $d_1 - d_2$ was sampled from −1.20 to 1.50 Å and RC2 = $d_3 - d_4$ was sampled from −1.80 to 1.20 Å. The umbrella windows were spaced in steps of 0.1 Å. Five picoseconds of relaxation were carried out in each windows followed by 10 ps of production with a time step of 0.5 fs. The values of the RC1 and RC2 were restrained to their target values with a harmonic potential and a force constant of 200.0 kcal/(mol·Å^2). The PMFs were unbiased using the 2D weighted histogram analysis method (WHAM-2D)[53] written by Alan Grossfield. The PMFs were later corrected by performing single point DFT/MM energies (see Supporting Information for details).

Scheme 2. Schematic Representation of the Reaction Coordinates Used to Simulate the First Half-Reaction Catalyzed by the Class 1A from *L. lactis* DHOD

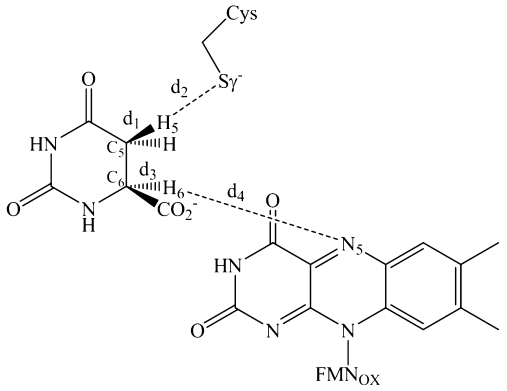

Interaction Energy Decomposition. We have carried out an energy decomposition analysis to study how active site residues stabilize/destabilize the transition state versus the Michaelis complex. The method was used before in studies of enzymatic systems.[28,34,37,54−58]

For a given structure, a residue is mutated to a glycine, and the energies recalculated. Equation 1 represents the influence of a residue's side chain to the energy by taking the difference between the energies when a particular residue is present (named by i in eq 1) or when it is mutated to Gly ($i - 1$ in eq 1).[59,60]

$$\Delta E_i = [E_i^{QM} + E_i^{QM/MM}] - [E_{i-1}^{QM} + E_{i-1}^{QM/MM}] \quad (1)$$

It should be noted that while the quantity above is usually referred to as the interaction energy, it also contains a term due to the change in QM energy itself. We estimated the relative stabilization due to the mutation between MC and TS for each residue as

$$\Delta\Delta E_i = \Delta E_i^{TS} - \Delta E_i^{MC} \quad (2)$$

The QM subsystem included the substrate, the cofactor, and the nucleophile Cys130. The values from eqs 1 and 2 were averaged over 100 snapshots from the QM/MM MD, using

DOI: 10.1021/jp512860r
J. Phys. Chem. B 2015, 119, 1468−1473

coordinates taken from the umbrella simulations at the MC and the TS.

A positive (negative) value of $\Delta\Delta E_i$ means that the side chain of residue i has a higher destabilization (stabilization) electrostatic effect on the TS than on the MC.

RESULTS AND DISCUSSION

Protonation State for Catalytic Base in *L. lactis* DHOD. The shifts of pK_a values of residues in enzymatic mechanisms has been highlighted.[58,61−67] Cys130 has been identified in class 1A DHODs as a general catalytic base, which has previously been reported in experimental studies.[1,2,13−15] The DHODs catalytic site does not perturb the electrostatic field to deprotonate the thiol group of Cys130. Inaoka et al. proposed that a water molecule could support the deprotonation of Cys130.[24] Norager et al. proposed that when the substrate enters the pocket, the thiol group could form a hydrogen bond with the carboxylate group of the DHO, allowing for deprotonation of the Cysteine.[68] However, in previous theoretical results there is no hydrogen bond formed between the carboxylate group and Cys130 amino acid.[19] Then in accordance with Inaoka's publication,[24] we kept the thiol group of Cys130 deprotonated.

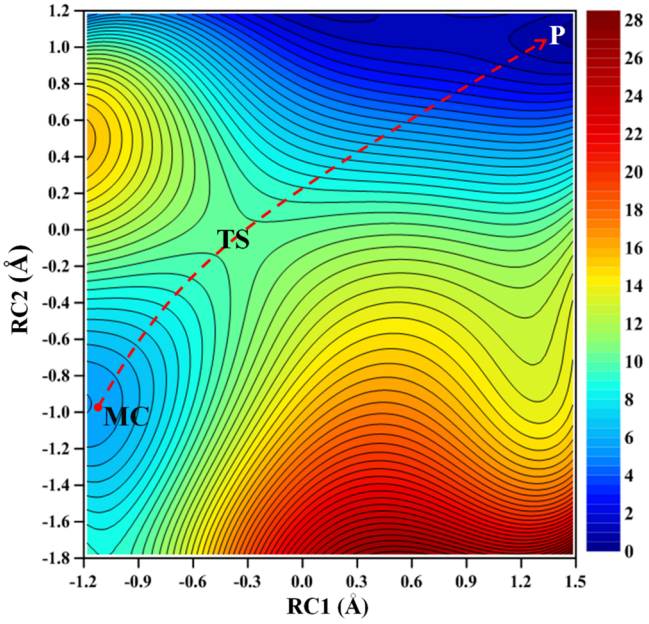

Figure 1. Two-dimensional FES obtained for the first half-reaction catalyzed by *L. lactis* DHOD using SCC-DFTB/MM level. The energy values are reported in kcal/mol.

Table 1. Relevant Distances (in Å) and Their Standard Deviation (in Parentheses) for MC, TS, and PROD Structures for the First Half-Reaction (DHO Oxidation) Obtained by SCC-DFTB/MM Level

SCC-DFTB/MM	MC	TS	PROD
$d(C_5 - H_5)$	1.13 (0.03)	1.48 (0.04)	2.85 (0.06)
$d(H_5 - S_\gamma)$	2.33 (0.05)	1.49 (0.04)	1.35 (0.04)
$d(C_6 - H_6)$	1.13 (0.03)	1.28 (0.03)	2.24 (0.05)
$d(H_6 - N_5)$	2.13 (0.04)	1.34 (0.04)	1.03 (0.02)

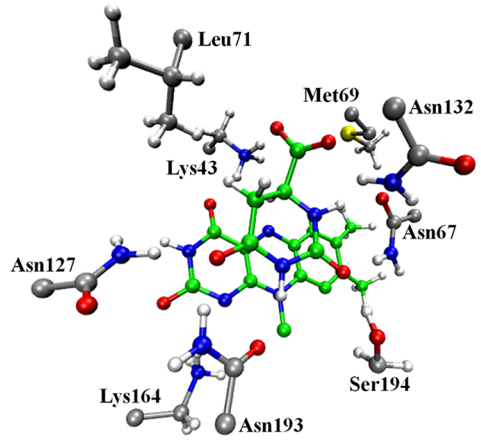

Figure 3. Representative structure of the MC considered on the residual decomposition analysis.

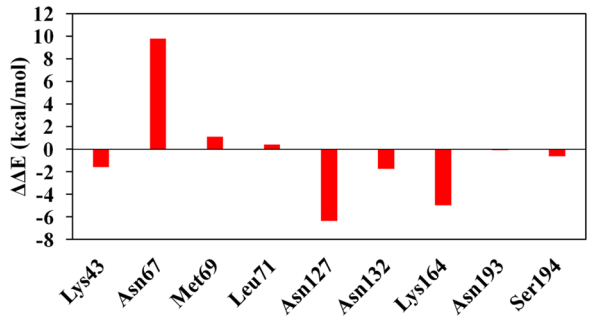

Figure 4. Stabilization of the TS with respect to the MC by active site residues.

QM/MM Umbrella Sampling and 2D Free Energy Surface (FES). The 2D free energy surface for the oxidation of DHO by *L. lactis* DHOD is shown in Figure 1. According to the results, there are two different changes. During the proton transfer from DHO to the catalytic residue Cys130, the $d(C_5-H_5)$ bond changes from 1.13 Å in the MC to 1.48 Å in the transition state (TS) and then to 2.85 Å in products (PROD);

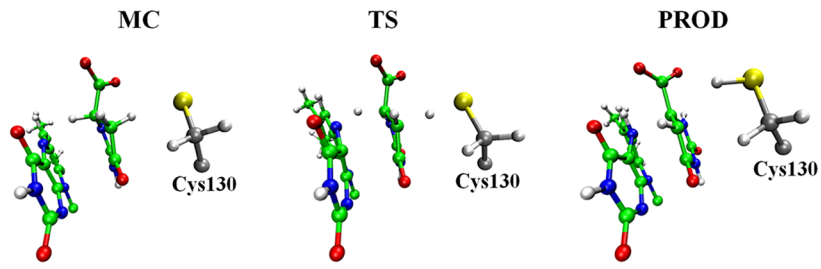

Figure 2. Representative snapshots of the MC, TS, and PROD.

DOI: 10.1021/jp512860r
J. Phys. Chem. B 2015, 119, 1468−1473

simultaneously, the $d(H_5-S_\gamma)$ bond decreases from 2.33 Å in the MC to 1.49 Å in TS and then to 1.35 Å in PROD (Figure 2). There is also a transfer of a hydride (H_6) from DHO C_6 to FMN N_5, where the distances $d(C_6-H_6)$ and $d(H_6-N_5)$ respectively change from 1.13 and 2.13 Å in MC complex to 1.28 and 1.34 Å in TS, and then to 2.24 and 1.03 Å in PROD (Figure 2). All these distances and their standard deviations are reported in Table 1.

In terms of energetics, the calculated energy barrier ($\Delta G^{\ddagger}_{r}$) is 5.64 kcal/mol, which rationalizes the experimental evidence that identifies DHOD as a very fast enzyme (fast enough that the experimental procedures are carried out at low temperatures to be measurable[69]). The free energy barrier obtained by the corrected PMFs using DFT/MM method is 5.06 kcal/mol, showing the SCC-DFTB/MM is in good agreement to high theory level as DFT. The computed ΔG°_{r} for the reaction is −3.90 kcal/mol making the reaction from DHOD-DHO to DHOD-OA complex thermodynamically favorable. In the literature, there is a considerable discussion as to whether the mechanism occurs in a stepwise or a concerted manner.[13,16,24] Previous theoretical results at the AM1/MM level showed that DHO oxidation catalyzed by DHOD from *T. cruzi* occurs via a concerted mechanism.[19] Our current results clearly show that the oxidation of DHO by the class 1A DHOD enzyme from *L. lactis* occurs via a concerted mechanism, which is in agreement with experiments.[13]

Energy Decomposition Analysis. The energy decomposition method was used to identify the effect of active site residues on the energy barrier of the first half-reaction catalyzed by *L. lactis* DHOD (Figure 3). Results are presented in Figure 4. The overall value was −4.11 kcal/mol, resulting in a reasonable stabilizing effect on the TS. Interestingly, Asn67 has a destabilizing effect on the TS, counteracted by the stabilizing the stabilizing effect exerted by residues Lys43, Asn127, Asn132, and Lys164. Residues Asn127 and Asn132 interact through hydrogen bonds with DHO and have a stabilizing effect on the TS of −6.35 and −1.75 kcal/mol, respectively. Residues Lys43 and Lys164 interact through hydrogen bonds with the FMN, stabilizing the TS. The side chain of Lys43 interacts with the N_5 atom of FMN; this interaction has a direct relation with hydride transfer during the oxidation step. The side chain of Lys164 interacts with the isoalloxazine ring of FMN, stabilizing the negative charge deposited in the ring. The interactions that the Lys residues exert in the FMN are important, since the enzymatic function of flavoenzymes, such as DODH, highly depend on the flavin group surroundings.[2] The interaction of Lys43 with the flavin group of FMN has not been reported for others flavoenzymes and may be a crucial feature in the behavior of class 1A DHODs, as highlighted experimentally.[2]

CONCLUSIONS

We present results for the mechanism of the first half-reaction in *L. lactis* DHOD using SCC-DFTB/MM umbrella sampling simulations and 2D PMFs calculations. Our results show that in the first half-reaction where the breaking and forming of the required bonds occurs via a concerted route. The computed free energy barrier for the half-reaction is very low, 5.64 kcal/mol, consistent with the available experimental evidence. The importance of residues Lys43, Asn127, Asn132, and Lys164 in stabilizing the TS during the redox reaction are highlighted through our analysis.

ASSOCIATED CONTENT

Supporting Information

Details of the barrier free energy correction by B3LYP/MM. This material is available free of charge via the Internet at http://pubs.acs.org.

AUTHOR INFORMATION

Corresponding Authors

*E-mail: roitberg@ufl.edu. Phone: (352) 392-6972. Fax: (352) 392-8722.

*E-mail: nahum@ufpa.br. Phone: (+55) 91-3201-8235. Fax: (+55) 91-3201-7633.

Author Contributions

The manuscript was written through contributions of all authors. All authors have given approval to the final version of the manuscript. All authors contributed equally.

Notes

The authors declare no competing financial interest.

ACKNOWLEDGMENTS

We gratefully acknowledge financial support from Conselho Nacional de Desenvolvimento Científico e Tecnológico from Brazil (CNPq). J.R.A.S. and C.N.A thank the Coordenação de Aperfeiçoamento de Pessoal de Nível Superior (CAPES) for financial support. The authors thank the University of Florida Research Computing for generous allotment of computer time. We thank Justin Smith for the corrections and suggestions that helped improve the readability of this manuscript.

REFERENCES

(1) Bjornberg, O.; Rowland, P.; Larsen, S.; Jensen, K. F. Active Site of Dihydroorotate Dehydrogenase A from Lactococcus Lactis Investigated by Chemical Modification and Mutagenesis. *Biochemistry* **1997**, *36*, 16197−16205.

(2) Rowland, P.; Bjornberg, O.; Nielsen, F. S.; Jensen, K. F.; Larsen, S. The Crystal Structure of Lactococcus Lactis Dihydroorotate Dehydrogenase A Complexed with the Enzyme Reaction Product Throws Light on Its Enzymatic Function. *Protein Sci.* **1998**, *7*, 1269−1279.

(3) Weber, G. Biochemical Strategy of Cancer-Cells and the Design of Chemotherapy-Gha-Clowes-Memorial-Lecture. *Cancer Res.* **1983**, *43*, 3466−3492.

(4) Elliott, W. L.; Sawick, D. P.; Defrees, S. A.; Heinstein, P. F.; Cassady, J. M.; Morre, D. J. Cyclic Modulation of Enzymes of Pyrimidine Nucleotide Biosynthesis Precedes Sialoglycoconjugate Changes During 2-Acetylaminofluorene-Induced Hepatocarcinogenesis in the Rat. *Biochim. Biophys. Acta* **1984**, *800*, 194−201.

(5) Breedveld, F. C.; Dayer, J. M. Leflunomide: Mode of Action in the Treatment of Rheumatoid Arthritis. *Ann. Rheum. Dis.* **2000**, *59*, 841−849.

(6) Palfey, B. A.; Bjornberg, O.; Jensen, F. Specific Inhibition of a Family 1A Dihydroorotate Dehydrogenase by Benzoate Pyrimidine Analogues. *J. Med. Chem.* **2001**, *44*, 2861−2864.

(7) Cherwinski, H. M.; Byars, N.; Ballaron, S. J.; Nakano, G. M.; Young, J. M.; Ransom, J. T. Leflunomide Interferes with Pyrimidine Nucleotide Biosynthesis. *Inflammation Res.* **1995**, *44*, 317−322.

(8) Cherwinski, H. M.; Cohn, R. G.; Cheung, P.; Webster, D. J.; Xu, Y. Z.; Caulfield, J. P.; Young, J. M.; Nakano, G.; Ransom, J. T. The Immunosuppressant Leflunomide Inhibits Lymphocyte-Proliferation by Inhibiting Pyrimidine Biosynthesis. *J. Pharmacol. Exp. Ther.* **1995**, *275*, 1043−1049.

(9) Nielsen, F. S.; Rowland, P.; Larsen, S.; Jensen, K. F. Purification and Characterization of Dihydroorotate Dehydrogenase A from Lactococcus Lactis, Crystallization and Preliminary X-Ray Diffraction Studies of the Enzyme. *Protein Sci.* **1996**, *5*, 852−856.

DOI: 10.1021/jp512860r
J. Phys. Chem. B 2015, 119, 1468−1473

(10) Nagy, M.; Lacroute, F.; Thomas, D. Divergent Evolution of Pyrimidine Biosynthesis Between Anaerobic and Aerobic Yeasts. *Proc. Natl. Acad. Sci. U.S.A.* **1992**, *89*, 8966−8970.
(11) Liu, S. P.; Neidhardt, E. A.; Grossman, T. H.; Ocain, T.; Clardy, J. Structures of Human Dihydroorotate Dehydrogenase in Complex with Antiproliferative Agents. *Structure* **2000**, *8*, 25−33.
(12) Rowland, P.; Nielsen, F. S.; Jensen, K. F.; Larsen, S. The Crystal Structure of the Flavin Containing Enzyme Dihydroorotate Dehydrogenase A From Lactococcus Lactis. *Structure* **1997**, *5*, 239−252.
(13) Fagan, R. L.; Jensen, K. F.; Bjornberg, O.; Palfey, B. A. Mechanism of Flavin Reduction in the Class 1A Dihydroorotate Dehydrogenase from Lactococcus Lactis. *Biochemistry* **2007**, *46*, 4028−4036.
(14) Bjornberg, O.; Jordan, D. B.; Palfey, B. A.; Jensen, K. F. Dihydrooxonate is a Substrate of Dihydroorotate Dehydrogenase (DHOD) Providing Evidence for Involvement of Cysteine and Serine Residues in Base Catalysis. *Arch. Biochem. Biophys.* **2001**, *391*, 286−294.
(15) Norager, S.; Arent, S.; Bjornberg, O.; Ottosen, M.; Lo Leggio, L.; Jensen, K. F.; Larsen, S. Lactococcus Lactis Dihydroorotate Dehydrogenase A Mutants Reveal Important Facets of the Enzymatic Function. *J. Biol. Chem.* **2003**, *278*, 28812−28822.
(16) Fagan, R. L.; Nelson, M. N.; Pagano, P. M.; Palfey, B. A. Mechanism of Flavin Reduction in Class 2 Dihydroorotate Dehydrogenases. *Biochemistry* **2006**, *45*, 14926−14932.
(17) Rowland, P.; Norager, S.; Jensen, K. F.; Larsen, S. Structure of Dihydroorotate Dehydrogenase B: Electron Transfer Between Two Flavin Groups Bridged by an Iron-Sulphur Cluster. *Structure* **2000**, *8*, 1227−1238.
(18) Fagan, R. L.; Palfey, B. A. Roles in Binding and Chemistry for Conserved Active Site Residues in the Class 2 Dihydroorotate Dehydrogenase from Escherichia Coli. *Biochemistry* **2009**, *48*, 7169−7178.
(19) Silva, N. d. F.; Lameira, J.; Alves, C. N.; Marti, S. Computational Study of the Mechanism of Half-Reactions in Class 1A Dihydroorotate Dehydrogenase from Trypanosoma Cruzi. *Phys. Chem. Chem. Phys.* **2013**, *15*, 18863−18871.
(20) Munier-Lehmann, H.; Vidalain, P.-O.; Tangy, F.; Janin, Y. L. On Dihydroorotate Dehydrogenases and Their Inhibitors and Uses. *J. Med. Chem.* **2013**, *56*, 3148−3167.
(21) Cheleski, J.; Rocha, J. R.; Pinheiro, M. P.; Wiggers, H. J.; da Silva, A. B. F.; Nonato, M. C.; Montanari, C. A. Novel Insights for Dihydroorotate Dehydrogenase Class 1A Inhibitors Discovery. *Eur. J. Med. Chem.* **2010**, *45*, 5899−5909.
(22) Cheleski, J.; Wiggers, H. J.; Citadini, A. P.; da Costa Filho, A. J.; Nonato, M. C.; Montanari, C. A. Kinetic Mechanism and Catalysis of Trypanosoma Cruzi Dihydroorotate Dehydrogenase Enzyme Evaluated by Isothermal Titration Calorimetry. *Anal. Biochem.* **2010**, *399*, 13−22.
(23) Cordeiro, A. T.; Feliciano, P. R.; Pinheiro, M. P.; Cristina Nonato, M. Crystal Structure of Dihydroorotate Dehydrogenase from Leishmania Major. *Biochimie* **2012**, *94*, 1739−1748.
(24) Inaoka, D. K.; Sakamoto, K.; Shimizu, H.; Shiba, T.; Kurisu, G.; Nara, T.; Aoki, T.; Kita, K.; Harada, S. Structures of Trypanosoma Cruzi Dihydroorotate Dehydrogenase Complexed with Substrates and Products: Atomic Resolution Insights Into Mechanisms of Dihydroorotate Oxidation and Fumarate Reduction. *Biochemistry* **2008**, *47*, 10881−10891.
(25) Warshel, A.; Levitt, M. Theoretical Studies of Enzymic Reactions-Dielectric, Electrostatic and Steric Stabilization of Carbonium-Ion in Reaction of Lysozyme. *J. Mol. Biol.* **1976**, *103*, 227−249.
(26) Marti, S.; Andres, J.; Moliner, V.; Silla, E.; Tunon, I.; Bertran, J. Computational Design of Biological Catalysts. *Chem. Soc. Rev.* **2008**, *37*, 2634−2643.
(27) Ruiz-Pernia, J. J.; Silla, E.; Tunon, I.; Marti, S. Hybrid Quantum Mechanics/Molecular Mechanics Simulations with Two-Dimensional Interpolated Corrections: Application to Enzymatic Processes. *J. Phys. Chem. B* **2006**, *110*, 17663−17670.
(28) Pierdominici-Sottile, G.; Horenstein, N. A.; Roitberg, A. E. Free Energy Study of the Catalytic Mechanism of Trypanosoma Cruzi Trans-Sialidase. From the Michaelis Complex to the Covalent Intermediate. *Biochemistry* **2011**, *50*, 10150−10158.
(29) Reis, M.; Alves, C. N.; Lameira, J.; Tunon, I.; Marti, S.; Moliner, V. The Catalytic Mechanism of Glyceraldehyde 3-Phosphate Dehydrogenase from Trypanosoma Cruzi Elucidated Via the QM/MM Approach. *Phys. Chem. Chem. Phys.* **2013**, *15*, 3772−3785.
(30) van der Kamp, M. W.; Mulholland, A. J. Combined Quantum Mechanics/Molecular Mechanics (QM/MM) Methods in Computational Enzymology. *Biochemistry* **2013**, *52*, 2708−2728.
(31) Senn, H. M.; Thiel, W. QM/MM Methods for Biomolecular Systems. *Angew. Chem., Int. Ed.* **2009**, *48*, 1198−1229.
(32) Field, M. J.; Albe, M.; Bret, C.; Proust-De Martin, F.; Thomas, A. The Dynamo Library for Molecular Simulations Using Hybrid Quantum Mechanical and Molecular Mechanical Potentials. *J. Comput. Chem.* **2000**, *21*, 1088−1100.
(33) Rosta, E.; Klahn, M.; Warshel, A. Towards Accurate Ab Initio QM/MM Calculations of Free-Energy Profiles of Enzymatic Reactions. *J. Phys. Chem. B* **2006**, *110*, 2934−2941.
(34) Bueren-Calabuig, J. A.; Pierdominici-Sottile, G.; Roitberg, A. E. Unraveling the Differences of the Hydrolytic Activity of Trypanosoma Cruzi Trans-Sialidase and Trypanosoma Rangeli Sialidase: A Quantum Mechanics-Molecular Mechanics Modeling Study. *J. Phys. Chem. B* **2014**, *118*, 5807−5816.
(35) Lameira, J.; Alves, C. N.; Tunon, I.; Marti, S.; Moliner, V. Enzyme Molecular Mechanism as a Starting Point to Design New Inhibitors: A Theoretical Study of O-GIcNAcase. *J. Phys. Chem. B* **2011**, *115*, 6764−6775.
(36) Alves, C. N.; Marti, S.; Castillo, R.; Andres, J.; Moliner, V.; Tunon, I.; Silla, E. A Quantum Mechanic/Molecular Mechanic Study of the Wild-Type and N155S Mutant HIV-1 Integrase Complexed with Diketo Acid. *Biophys. J.* **2008**, *94*, 2443−2451.
(37) Silva, J. R. A.; Roitberg, A. E.; Alves, C. N. Catalytic Mechanism of L,D-Transpeptidase 2 from Mycobacterium tuberculosis Described by a Computational Approach: Insights for the Design of New Antibiotics Drugs. *J. Chem. Inf. Model.* **2014**, *54*, 2402−2410.
(38) Warshel, A. Computer Simulations of Enzyme Catalysis: Methods, Progress, and Insights. *Annu. Rev. Biophys. Biomol. Struct.* **2003**, *32*, 425−443.
(39) Kruger, T.; Elstner, M.; Schiffels, P.; Frauenheim, T. Validation of the Density-Functional Based Tight-Binding Approximation Method for the Calculation of Reaction Energies and Other Data. *J. Chem. Phys.* **2005**, *122*, 114110−114114.
(40) Woodcock, H. L.; Hodoscek, M.; Brooks, B. R. Exploring SCC-DFTB Paths for Mapping QM/MM Reaction Mechanisms. *J. Phys. Chem. A* **2007**, *111*, 5720−5728.
(41) Barnett, C. B.; Naidoo, K. J. Ring Puckering: A Metric for Evaluating the Accuracy of AM1, PM3, PM3CARB-1, and SCC-DFTB Carbohydrate QM/MM Simulations. *J. Phys. Chem. B* **2010**, *114*, 17142−17154.
(42) Li, H.; Robertson, A. D.; Jensen, J. H. Very Fast Empirical Prediction and Rationalization af Protein Pk(a) Values. *Proteins* **2005**, *61*, 704−721.
(43) Case, D.; Darden, T. A.; Cheatham, T. E.; Simmerling, C.; Wang, J.; Duke, R.; Luo, R.; Crowley, M.; Walker, R.; Zhang, W.; et al. *AMBER 12*; University of California: San Francisco, 2012.
(44) Jorgensen, W. L.; Chandrasekhar, J.; Madura, J. D.; Impey, R. W.; Klein, M. L. Comparison of Simple Potential Functions for Simulating Liquid Water. *J. Chem. Phys.* **1983**, *79*, 926−935.
(45) Hornak, V.; Abel, R.; Okur, A.; Strockbine, B.; Roitberg, A.; Simmerling, C. Comparison of Multiple Amber Force Fields and Development of Improved Protein Backbone Parameters. *Proteins* **2006**, *65*, 712−725.
(46) Wang, J. M.; Wolf, R. M.; Caldwell, J. W.; Kollman, P. A.; Case, D. A. Development and Testing of a General Amber Force Field. *J. Comput. Chem.* **2004**, *25*, 1157−1174.
(47) Frisch, M. J.; Trucks, G. W.; Schlegel, H. B.; Scuseria, G. E.; Robb, M. A.; Cheeseman, J. R.; Scalmani, G.; Barone, V.; Mennucci,

DOI: 10.1021/jp512860r
J. Phys. Chem. B 2015, 119, 1468−1473

B.; Petersson, G. A.; Nakatsuji, H.; Caricato, M.; Li, X.; Hratchian, H. P.; Izmaylov, A. F.; Bloino, J.; Zheng, G.; Sonnenberg, J. L.; Hada, M.; Ehara, M.; Toyota, K.; Fukuda, R.; Hasegawa, J.; Ishida, M.; Nakajima, T.; Honda, Y.; Kitao, O.; Nakai, H.; Vreven, T.; Montgomery, J. A., Jr.; Peralta, P. E.; Ogliaro, F.; Bearpark, M.; Heyd, J. J.; Brothers, E.; Kudin, K. N.; Staroverov, V. N.; Kobayashi, R.; Normand, J.; Raghavachari, K.; Rendell, A.; Burant, J. C.; Iyengar, S. S.; Tomasi, J.; Cossi, M.; Rega, N.; Millam, N. J.; Klene, M.; Knox, J. E.; Cross, J. B.; Bakken, V.; Adamo, C.; Jaramillo, J.; Gomperts, R.; Stratmann, R. E.; Yazyev, O.; Austin, A. J.; Cammi, R.; Pomelli, C.; Ochterski, J. W.; Martin, R. L.; Morokuma, K.; Zakrzewski, V. G.; Voth, G. A.; Salvador, P.; Dannenberg, J. J.; Dapprich, S.; Daniels, A. D.; Farkas, Ö.; Ortiz, J. V.; Cioslowski, J.; Fox, D. J. *Gaussian 09*, revision D.01; Gaussian, Inc.: Wallingford, CT, 2009.

(48) Schneider, C.; Suhnel, J. A Molecular Dynamics Simulation of the Flavin Mononucleotide-RNA Aptamer Complex. *Biopolymers* **1999**, *50*, 287−302.

(49) Ryckaert, J. P.; Ciccotti, G.; Berendsen, H. J. C. Numerical-Integration of Cartesian Equations of Motion of a System with Constraints-Molecular-Dynamics of N-Alkanes. *J. Comput. Phys.* **1977**, *23*, 327−341.

(50) Elstner, M.; Porezag, D.; Jungnickel, G.; Elsner, J.; Haugk, M.; Frauenheim, T.; Suhai, S.; Seifert, G. Self-Consistent-Charge Density-Functional Tight-Binding Method for Simulations of Complex Materials Properties. *Phys. Rev. B: Condens. Matter Mater. Phys.* **1998**, *58*, 7260−7268.

(51) Seabra, G. d. M.; Walker, R. C.; Elstner, M.; Case, D. A.; Roitberg, A. E. Implementation of the SCC-DFTB Method for Hybrid QM/MM Simulations Within the Amber Molecular Dynamics Package. *J. Phys. Chem. A* **2007**, *111*, 5655−5664.

(52) Field, M. J.; Bash, P. A.; Karplus, M. A Combined Quantum-Mechanical and Molecular Mechanical Potential for Molecular-Dynamics Simulations. *J. Comput. Chem.* **1990**, *11*, 700−733.

(53) Kumar, S.; Bouzida, D.; Swendsen, R. H.; Kollman, P. A.; Rosenberg, J. M. The Weighted Histogram Analysis Method for Free-Energy Calculations on Biomolecules 0.1. The Method. *J. Comput. Chem.* **1992**, *13*, 1011−1021.

(54) Chatfield, D. C.; Eurenius, K. P.; Brooks, B. R. HIV-1 Protease Cleavage Mechanism: A Theoretical Investigation Based on Classical MD Simulation and Reaction Path Calculations Using a Hybrid QM/MM Potential. *J. Mol. Struct.: THEOCHEM* **1998**, *423*, 79−92.

(55) Dinner, A. R.; Blackburn, G. M.; Karplus, M. Uracil-DNA Glycosylase Acts by Substrate Autocatalysis. *Nature* **2001**, *413*, 752−755.

(56) Garcia-Viloca, M.; Truhlar, D. G.; Gao, J. L. Reaction-Path Energetics and Kinetics of the Hydride Transfer Reaction Catalyzed by Dihydrofolate Reductase. *Biochemistry* **2003**, *42*, 13558−13575.

(57) Hensen, C.; Hermann, J. C.; Nam, K. H.; Ma, S. H.; Gao, J. L.; Holtje, H. D. A Combined QM/MM Approach to Protein-Ligand Interactions: Polarization Effects of The HIV-1 Protease on Selected High Affinity Inhibitors. *J. Med. Chem.* **2004**, *47*, 6673−6680.

(58) Pierdominici-Sottile, G.; Roitberg, A. E. Proton Transfer Facilitated by Ligand Binding. An Energetic Analysis of the Catalytic Mechanism of Trypanosoma Cruzi Trans-Sialidase. *Biochemistry* **2011**, *50*, 836−842.

(59) Major, D. T.; Gao, J. A Combined Quantum Mechanical and Molecular Mechanical Study of the Reaction Mechanism and Alpha-Amino Acidity in Alanine Racemase. *J. Am. Chem. Soc.* **2006**, *128*, 16345−16357.

(60) Wong, K.-Y.; Gao, J. The Reaction Mechanism of Paraoxon Hydrolysis by Phosphotriesterase from Combined QM/MM Simulations. *Biochemistry* **2007**, *46*, 13352−13369.

(61) Riccardi, D.; Schaefer, P.; Cui, Q. pK(a) Calculations in Solution and Proteins with QM/MM Free Energy Perturbation Simulations: A Quantitative Test of QM/MM Protocols. *J. Phys. Chem. B* **2005**, *109*, 17715−17733.

(62) Harris, T. K.; Turner, G. J. Structural Basis of Perturbed pK(a) Values of Catalytic Groups in Enzyme Active Sites. *IUBMB Life* **2002**, *53*, 85−98.

(63) McIntosh, L. P.; Hand, G.; Johnson, P. E.; Joshi, M. D.; Korner, M.; Plesniak, L. A.; Ziser, L.; Wakarchuk, W. W.; Withers, S. G. The pK(a) of the General Acid/Base Carboxyl Group of a Glycosidase Cycles During Catalysis: A C-13-NMR Study of Bacillus Circuluns Xylanase. *Biochemistry* **1996**, *35*, 9958−9966.

(64) Vocadlo, D. J.; Davies, G. J.; Laine, R.; Withers, S. G. Catalysis by Hen Egg-White Lysozyme Proceeds Via a Covalent Intermediate. *Nature* **2001**, *412*, 835−838.

(65) Phillips, D. C. Hen Egg-White Lysozyme Molecule. *Proc. Natl. Acad. Sci. U.S.A.* **1967**, *57*, 484−495.

(66) Zhou, M. M.; Davis, J. P.; Vanetten, R. L. Identification and Pk(a) Determination of the Histidine-Residues of Human Low-Molecular-Weight Phosphotyrosyl Protein Phosphatases - A Convenient Approach Using an Mlev-17 Spectral Editing Scheme. *Biochemistry* **1993**, *32*, 8479−8486.

(67) Chivers, P. T.; Prehoda, K. E.; Volkman, B. F.; Kim, B. M.; Markley, J. L.; Raines, R. T. Microscopic pK(a) Values of Escherichia Coli Thioredoxin. *Biochemistry* **1997**, *36*, 14985−14991.

(68) Norager, S.; Jensen, K. F.; Bjornberg, O.; Larsen, S. E-Coli Dihydroorotate Dehydrogenase Reveals Structural and Functional Distinctions Between Different Classes of Dihydroorotate Dehydrogenases. *Structure* **2002**, *10*, 1211−1223.

(69) McDonald, C. A.; Palfey, B. A. Substrate Binding and Reactivity Are Not Linked: Grafting a Proton-Transfer Network into a Class 1A Dihydroorotate Dehydrogenase. *Biochemistry* **2011**, *50*, 2714−2716.

DOI: 10.1021/jp512860r
J. Phys. Chem. B 2015, 119, 1468−1473